PERGAMON

International Journal of Solids and Structures 38 (2001) 8701–8722

INTERNATIONAL JOURNAL OF SOLIDS and STRUCTURES

www.elsevier.com/locate/ijsolstr

Large simple shear and torsion problems in kinematic hardening elasto-plasticity with logarithmic rate

O.T. Bruhns *, H. Xiao, A. Meyers

Institute of Mechanics, Ruhr-University Bochum, Gebäude IA, Raum 3/26, Universitätsstrasse 150, D-44780 Bochum, Germany

Received 10 October 2000; in revised form 7 March 2001

Abstract

Large simple shear and torsion problems in plasticity have been the object of a large number of papers. Sophisticated schemes have been developed (e.g. J. Appl. Mech. 50 (1983) 561) that overcome problems encountered (cf. e.g. J. Mech. Phys. Solids 48 (2000) 2231; Int. J. Solids Struct. 37 (2000) 5037). This paper substantially uses the logarithmic rate (Acta Mechanica 124 (1997a) 89), which is equally based on strong mathematical and physical principles and therefore may contrast to classical approaches of cited kinds.

Stress responses to large simple shear and torsional deformations in elastoplastic bodies are studied by applying the self-consistent kinematic hardening J_2-flow model based on the logarithmic tensor rate, recently established by these authors (Int. J. Plasticity 15 (1999) 479). The application of the logarithmic stress rate in the elastic rate equation of hypoelastic type results in an exact finite hyperelastic solution in terms of Hencky's logarithmic strain. The plastic solution is composed of two parts: the back stress and the effective stress (the Kirchhoff stress reduced by the back stress). It is shown that the evolution equation of the back stress with the logarithmic rate is integrable to deliver a closed-form relation between the back stress and Hencky's logarithmic strain and the current stress. Moreover, the effective stress is shown to be governed by a first-order nonlinear ordinary differential equation with a small dimensionless material parameter multiplying the highest derivative, for which the initial condition is related to the elastic–plastic transition and prescribed in terms of the just-mentioned small parameter. A singular perturbation solution for the just-mentioned equation is derived by utilizing the method of matched expansions. With the analytical solution derived, it is possible to make a detailed study of the coupling effect of material properties, including the elastic, yielding and hardening properties, on elastic–plastic responses. For the large deformations at issue, it is demonstrated that, merely with three commonly known classical material constants, i.e., the elastic shear modulus, the initial tensile yield stress and the hardening modulus, the simple kinematic hardening J_2-flow model with the logarithmic rate may supply satisfactory explanations for salient features of complex behaviour in experimental observation. © 2001 Elsevier Science Ltd. All rights reserved.

Keywords: Elastic–plastic material; Kinematic hardening; Finite strain; Logarithmic rate; Shear and torsion; Analytical perturbation solution

* Corresponding author. Tel.: +49-234-322-3080; fax: +49-234-321-4229.
E-mail address: bruhns@tm.bi.ruhr-uni-bochum.de (O.T. Bruhns).

0020-7683/01/$ - see front matter © 2001 Elsevier Science Ltd. All rights reserved.
PII: S0020-7683(01)00068-3

1. Introduction

To be consistent with objectivity requirements, objective Eulerian tensor rates, instead of the usual material time derivative, should be used in formulating Eulerian rate type elasto-plasticity models at large strain. There are a large variety of objective rates for consideration. Earlier, Zaremba–Jaumann rate was given prominence. Since the unexpected shear oscillation phenomena with monotonically increasing shearing strain were discovered by Lehmann (1972a,b), Dienes (1979) and Nagtegaal and de Jong (1982), and other, a number of Eulerian rate type elasto-plasticity models at large strain have been proposed using various definitions of stress rates different from Zaremba–Jaumann rate, such as Oldroyd rate, Cotter–Rivlin rate, Truesdell rate, and Green–Naghdi rate, etc. (see, e.g., Neale, 1981; Nemat-Nasser, 1983, 1992 and the relevant references therein for details; and Agah-Tehrani et al., 1987). Usually, the large simple shear problem, which characterizes the torsion problem of thin-walled cylindrical tubes in a sense of suitable approximation as shown later, is used to test and justify reasonableness and applicability of various models suggested, refer to, e.g., Lehmann (1972a,b), Bruhns (1973), Dienes (1979), Nagtegaal and de Jong (1982), Lee et al. (1983), Dafalias (1983), Loret (1983), Atluri (1984), Johnson and Bammann (1984), Moss (1984), Paulun and Pecherski (1985), Reed and Atluri (1985), Haupt and Tsakmakis (1986), Lubarda (1988), Metzger and Dubey (1987), Zbib and Aifantis (1988a,b), Szabó and Balla (1989), Tsakmakis and Haupt (1989), Yang et al. (1992), Xia and Ellyin (1993), Majors and Krempl (1994), Ning and Aifantis (1994a,b), Cho and Dafalias (1996), Dafalias (2000), Kuroda (1997, 1999), Kuroda and Tvergaard (2000), and many others. A detailed account of this aspect can also be found in Khan and Huang (1995).

However, Simo and Pister (1984) demonstrated that, with several commonly known stress rates, none of the corresponding widely used hypoelastic equations (see Eq. (2.2) given in Section 2) intended for elastic behaviour is exactly integrable to define an elastic relation, and any of them is thus incompatible with the definition of elasticity, in particular, hyperelasticity. This fact means that any of the Eulerian rate elasto-plasticity models with commonly known stress rates is *self-inconsistent* in the sense of characterizing elastic behaviour in nonlinear range.

Very recently, in Bruhns et al. (1999) new Eulerian rate type elasto-plasticity models have been established for elastic-perfect plasticity and elasto-plasticity with isotropic and kinematic hardening by utilizing the *logarithmic rate* (see, e.g., Xiao et al., 1997a). These models are shown to be *self-consistent* in the following sense: the hypoelastic equation intended for elastic behaviour is integrable to deliver an elastic, in particular hyperelastic, relation. In Xiao et al. (1999), it is proved that, in order to fulfil the just-stated self-consistency criterion, the logarithmic rate is the only choice among all objective corotational rates and other well-known non-corotational rates.

As a typical example for large strain responses of the foregoing new models, in this article we study the large torsion problem of elastoplastic thin-walled cylindrical tubes with fixed ends by applying the self-consistent J_2-flow model with the logarithmic rate. The large simple shear problem has been studied for kinematic hardening elasto-plasticity models with various kinds of stress rates, as mentioned before. However, only numerical results were supplied in the past, and it seems that satisfactory simulation of experimental results has not been achieved by means of usually considered classical models with various objective rates, as indicated by Reed and Atluri (1985). Here it will be seen that an analytical perturbation solution is available for unlimited large strain. With this analytical solution, it is possible to make a detailed study of the coupling effect of material properties, including the elastic, yielding and hardening properties, on elastic–plastic responses. For the deformation response at issue, it will be demonstrated that, merely with three commonly used classical material constants, i.e., the elastic shear modulus, the initial tensile yield stress and the hardening modulus, the linear kinematic hardening J_2-flow model with the logarithmic rate may supply satisfactory explanation for salient features of complex behaviour in experimental observation.

The main content of this article is arranged as follows. In Section 2, we supply the kinematic hardening elastoplastic J_2-flow model with the logarithmic rate. In Section 3, the large torsion problem of thin-walled cylindrical tubes is reduced to the large simple shear problem of rectangular plates, and the kinematic analysis of the two kinds of finite deformations is provided. In Section 4, the elastic solution and the condition for elastic–plastic transition are determined. It is shown that the application of the logarithmic stress rate in the elastic rate equation of hypoelastic type supplies an exact finite hyperelastic relation between Kirchhoff stress and Hencky's logarithmic strain, which is exactly the one discussed and advocated by Anand (1979, 1986). In Section 5, the plastic solution is determined, which is composed of two parts: the back stress and the effective stress (the Kirchhoff stress deviator reduced by the back stress). It is shown that the evolution equation of the back stress with the logarithmic rate is integrable to deliver an exact relation between the back stress and Hencky's logarithmic strain and the current stress. Moreover, the effective stress is shown to be governed by a first-order nonlinear ordinary differential equation with a small dimensionless material parameter multiplying the highest derivative, for which the initial condition is related to the elastic–plastic transition and prescribed in terms of the just-mentioned small parameter. A singular perturbation solution for the just-mentioned equation is derived by utilizing the method of matched expansions. Finally, in Section 6 the coupling effect of elastic, yielding and hardening properties is studied in detail and explanations for relevant experimental results are made, by virtue of the analytical solution obtained.

2. Kinematic hardening J_2-flow model with logarithmic rate

Formulating Eulerian rate type elasto-plasticity models at finite strains, the additive decomposition of the stretching or the Eulerian strain rate $\mathbf{D}$, among other things, is usually postulated (see, e.g., Neale, 1981; Nemat-Nasser, 1983, 1992; and Agah-Tehrani et al., 1987):

$$\mathbf{D} = \mathbf{D}^{\mathrm{e}} + \mathbf{D}^{\mathrm{p}}. \tag{2.1}$$

Then, the two parts $\mathbf{D}^{\mathrm{e}}$ and $\mathbf{D}^{\mathrm{p}}$ are, respectively, characterized by a rate type equation intended for elastic behaviour and a rate type equation for plastic behaviour. Most often, especially for metals etc., the following hypoelastic formulation for $\mathbf{D}^{\mathrm{e}}$, the elastic part of $\mathbf{D}$, is assumed:

$$\mathbf{D}^{\mathrm{e}} = \frac{1+\nu}{E}\overset{\circ}{\boldsymbol{\tau}}{}^{*} - \frac{\nu}{E}(\mathrm{tr}\dot{\boldsymbol{\tau}})\mathbf{I}. \tag{2.2}$$

Here ν and E are Poisson's ratio and Young's modulus in classical infinitesimal isotropic elasticity, $\mathbf{I}$ is the second-order identity tensor, and $\boldsymbol{\tau}$ the Kirchhoff stress, i.e.

$$\boldsymbol{\tau} = J\boldsymbol{\sigma} \tag{2.3}$$

with $\boldsymbol{\sigma}$ the Cauchy stress and J the volume ratio or the mass density ratio related to the initial and current states. Hence

$$J = \det \mathbf{F}, \tag{2.4}$$

where $\mathbf{F}$ is the deformation gradient. In Eq. (2.2), $\overset{\circ}{\boldsymbol{\tau}}{}^{*}$ is an objective rate of the stress $\boldsymbol{\tau}$.

On the other hand, the associated plasticity and normality postulate together lead to the following flow rule for the coupled elastic–plastic part, $\mathbf{D}^{\mathrm{p}}$, of $\mathbf{D}$:

$$\mathbf{D}^{\mathrm{p}} = \dot{\rho}\frac{\partial f}{\partial \boldsymbol{\tau}}, \tag{2.5}$$

where $\dot{\rho}$ is the plastic multiplier and f the yield function. As commonly done, a traceless stress-like tensor $\boldsymbol{\alpha}$, the back stress, is introduced to characterize the hardening behaviour. Then the yield function f is formulated as an isotropic scalar function of the stress $\boldsymbol{\tau}$ and the back stress $\boldsymbol{\alpha}$ etc. In particular, a yield function of von Mises type is widely used, which locates the yield surface in the following manner:

$$f = \sqrt{\mathrm{tr}(\boldsymbol{\tau}' - \boldsymbol{\alpha})^2} - \sqrt{\frac{2}{3}} J_0 \sigma_0 = 0, \tag{2.6}$$

where $\boldsymbol{\tau}'$ designates the deviatoric part of the Kirchhoff stress, J_0 is the volume ratio at yielding, and σ_0 is the initial tensile yield stress.

The evolution equation for the back stress $\boldsymbol{\alpha}$ is of Prager's form:

$$\overset{\circ}{\boldsymbol{\alpha}}{}^{*} = c\mathbf{D}^{\mathrm{p}} \tag{2.7}$$

where c is a hardening parameter.

For continued plastic flow, the stress $\boldsymbol{\tau}$ must stay on the yield surface. This is guaranteed by the consistency condition $\dot{f} = 0$. By using this condition the plastic multiplier $\dot{\rho}$ may be determined. Then, a kinematic hardening elastoplastic model with the stress rate $\overset{\circ}{\boldsymbol{\tau}}{}^{*}$ and $\overset{\circ}{\boldsymbol{\alpha}}{}^{*}$ may be established as follows:

$$\overset{\circ}{\boldsymbol{\tau}}{}^{*} = 2\mu\mathbf{D} + \lambda\overline{\dot{\ln J}}\mathbf{I} - \frac{2\mu}{c + 2\mu}\frac{3\mu}{J_0^2\sigma_0^2}(\boldsymbol{\chi} : \mathbf{D})\boldsymbol{\chi}, \tag{2.8}$$

$$\overset{\circ}{\boldsymbol{\alpha}}{}^{*} = \frac{c}{c + 2\mu}\frac{3\mu}{J_0^2\sigma_0^2}(\boldsymbol{\chi} : \mathbf{D})\boldsymbol{\chi}, \tag{2.9}$$

where the loading/unloading condition is described e.g. by the Kuhn–Tucker relation

$$\dot{\rho} \geqslant 0, \quad f \leqslant 0, \quad \text{and} \quad \dot{\rho} f \equiv 0,$$

and $\boldsymbol{\chi}$, the effective stress, is defined as

$$\boldsymbol{\chi} = \boldsymbol{\tau}' - \boldsymbol{\alpha}. \tag{2.10}$$

Moreover, the Lamé elastic constants λ and μ are related to v and E by

$$2\mu = \frac{E}{1 + v}, \quad \lambda = \frac{vE}{(1 + v)(1 - 2v)}.$$

Evidently, a choice of the objective tensor rate $\overset{\circ}{\mathbf{A}}{}^{*}$ defines a kinematic hardening elasto-plasticity model of the above type. There are many (actually infinitely many; see, e.g., Xiao et al., 1998a,b) possible choices for the former. Earlier, a common choice was the well-known Zaremba–Jaumann rate

$$\overset{\circ}{\mathbf{A}}{}^{J} = \dot{\mathbf{A}} + \mathbf{A}\mathbf{W} - \mathbf{W}\mathbf{A}$$

with the vorticity tensor $\mathbf{W}$, the antisymmetric part of the velocity gradient. However, Lehmann (1972a,b), Dienes (1979) and Nagtegaal and de Jong (1982) disclosed that elasto-plasticity and hypoelasticity models with Zaremba–Jaumann rate predict oscillatory shear stress responses with increasing shear strain. These spurious oscillation phenomena prompted reexamination of basic aspects underlying large strain elasto-plastic models, including the validity of the decomposition (2.1), the definition of an appropriate stress rate $\overset{\circ}{\boldsymbol{\tau}}{}^{*}$, etc. In the latter aspect, several stress rates have been taken into account. Among them are Oldroyd rate, Cotter–Rivlin rate, Truesdell rate, and Green–Naghdi rate, etc. Elasto-plasticity models with these stress rates have been examined and compared for finite simple shear responses and other responses in order to test their reasonableness and applicability (see the relevant references mentioned before).

The above situation becomes rather complicated due to the following fact: it seems not easy even to establish whether a given model is reasonable or not in a full sense, let alone consider and compare the

infinite many possible models, as pointed out before. Very recently, an attempt has been made to clarify this situation. The present authors (Bruhns et al., 1999; Xiao et al., 1999) have introduced the following self-consistency criterion necessary for any reasonable elasto-plasticity model: For every process of purely elastic deformation, i.e. for $\mathbf{D} = \mathbf{D}^{\mathrm{e}}$, the commonly used hypoelastic equation (2.2) intended for elastic behaviour must be exactly integrable to really deliver a hyperelastic relation. In the just-mentioned references it is proved that, among all Eulerian rate type elasto-plasticity models with all infinitely many corotational stress rates and other known stress rates, only those with the logarithmic rate $\overset{\circ}{\boldsymbol{\tau}}{}^{\log}$ fulfil the just-stated self-consistency criterion (Xiao et al., 1997a, 1998a,b). For the models of the form (2.8) and (2.9), this fact results in the unique self-consistent kinematic hardening elasto-plasticity model (cf. Eqs. (93), (94) and (96) in Bruhns et al., 1999; note that the total volumetric deformation is elastic):

$$\mathrm{tr}\boldsymbol{\tau} = \frac{E}{1-2\nu}\ln J, \tag{2.11}$$

$$\overset{\circ}{\boldsymbol{\tau}}{}^{\log} = 2\mu\mathbf{D} + \lambda\overline{\ln J}\,\mathbf{I} - \frac{2\mu}{c+2\mu}\frac{3\mu}{J_0^2\sigma_0^2}(\boldsymbol{\chi}:\mathbf{D})\boldsymbol{\chi}, \tag{2.12}$$

$$\overset{\circ}{\boldsymbol{\alpha}}{}^{\log} = \frac{c}{c+2\mu}\frac{3\mu}{J_0^2\sigma_0^2}(\boldsymbol{\chi}:\mathbf{D})\boldsymbol{\chi}, \tag{2.13}$$

where the logarithmic rate $\overset{\circ}{\mathbf{A}}{}^{\log}$ of a second-order symmetric tensor $\mathbf{A}$ is defined by

$$\overset{\circ}{\mathbf{A}}{}^{\log} = \dot{\mathbf{A}} + \mathbf{A}\boldsymbol{\Omega}^{\log} - \boldsymbol{\Omega}^{\log}\mathbf{A} \tag{2.14}$$

with the logarithmic spin

$$\boldsymbol{\Omega}^{\log} = \mathbf{W} + \sum_{\sigma\neq\tau}^{m}\left(\frac{1+\frac{b_\sigma}{b_\tau}}{1-\frac{b_\sigma}{b_\tau}} + \frac{2}{\ln\frac{b_\sigma}{b_\tau}}\right)\mathbf{B}_\sigma\mathbf{D}\mathbf{B}_\tau. \tag{2.15}$$

Here and in Eq. (3.6) given later, $b_1, \ldots, b_m$ are the distinct eigenvalues of the left Cauchy–Green tensor $\mathbf{B} = \mathbf{F}\mathbf{F}^{\mathrm{T}}$ and $\mathbf{B}_1, \ldots, \mathbf{B}_m$ the corresponding subordinate eigenprojections of $\mathbf{B}$. An explicit basis-free expression for $\boldsymbol{\Omega}^{\log}$ can be found in Xiao et al. (1997a, 1998a,b).

We conclude this section with a useful relation concerning the logarithmic rate. The second-order skewsymmetric tensor $\mathbf{R}^{\log}$ defined by the tensorial differential equation

$$\overline{\dot{\mathbf{R}}^{\log}} = -\mathbf{R}^{\log}\boldsymbol{\Omega}^{\log} \tag{2.16}$$

with the initial condition

$$(\mathbf{R}^{\log})|_{t=0} = \mathbf{I} \tag{2.17}$$

is called the *logarithmic rotation*. The following relation holds (see, Bruhns et al., 1999):

$$\mathbf{R}^{\log}\bigstar\overset{\circ}{\mathbf{A}}{}^{\log} = \overline{\dot{(\mathbf{R}^{\log}\bigstar\mathbf{A})}}. \tag{2.18}$$

In particular, we have

$$\mathbf{R}^{\log}\bigstar\mathbf{D} = \overline{\dot{(\mathbf{R}^{\log}\bigstar\ln\mathbf{V})}}. \tag{2.19}$$

In the latter, $\ln\mathbf{V}$ is the Hencky's logarithmic strain that will be defined by Eq. (3.6). Here and henceforth,

$$\mathbf{R}^{\log}\bigstar\mathbf{A} = \mathbf{R}^{\log}\mathbf{A}(\mathbf{R}^{\log})^{\mathrm{T}}.$$

3. Large torsion and large simple shear deformations

Consider a cylindrical tube with the average radius R and the thickness δ. Let the two ends of the tube be fixed. With the torque M at the two ends applied, each cross-section of the tube under consideration will be twisted through an angle along its central axial line. The angle of twist per unit length is denoted by ψ.

There are lower and upper limits M_1 and M_2 for the torque M. When the applied torque M does not exceed the lower limit M_1, the whole tube will be in the elastic state. For a torque $M_1 \leqslant M \leqslant M_2$, an elastic–plastic boundary surface will divide the tube into two parts: the outer part is plastically deformed, while the inner part remains in the elastic state. Once the torque M exceeds the upper limit M_2, the whole tube will be in the plastic state.

Generally, it does not appear to be easy to determine the stress components in the tube at large torsion. However, when the thickness δ is very small, in a sense of approximation the stress and strain states in the whole tube may be assumed to be homogeneous and represented by those at the mid-surface of the tube.

With the above approximation of homogenization the whole thin-walled tube undergoes simple shear deformation. As a result, the large torsion problem of thin-walled tubes with fixed ends is reduced to the large simple shear problem of thin rectangular plates. The latter will be treated below.

Choose a fixed Cartesian rectangular coordinate system (O, X_1, X_2, X_3) in the mid-plane of a rectangular plate with the origin O a corner point of the mid-plane and the fixed X_1-, X_2- and X_3-axes along the directions of two edges and the normal direction of the mid-plane, respectively. To correspond with the torsion of the aforementioned cylindrical tube, one may regard the plate to be a small element cut out of the tube in such a manner that the X_2-axis and X_3-axis are along the central axial line of the tube and the radial direction of the tube. The simple shear deformation of the plate is described by

$$\mathbf{x} = (X_1 + \gamma X_2)\mathbf{e}_1 + X_2\mathbf{e}_2 + X_3\mathbf{e}_3. \tag{3.1}$$

In the above, $(\mathbf{e}_1, \mathbf{e}_2, \mathbf{e}_3)$ are three orthonormal vectors along the three fixed coordinate axes mentioned before, and $\mathbf{X} = \sum_{i=1}^{3} X_i\mathbf{e}_i$ and $\mathbf{x} = \sum_{i=1}^{3} x_i\mathbf{e}_i$ are the initial and the current position vectors of a material particle in the plate. Moreover, the shear strain γ is related to the angle of twist, ψ, by

$$\gamma = R\psi. \tag{3.2}$$

The left Cauchy–Green tensor $\mathbf{B}$ is of the form

$$\mathbf{B} = (1 + \gamma^2)\mathbf{e}_1 \otimes \mathbf{e}_1 + \gamma(\mathbf{e}_1 \otimes \mathbf{e}_2 + \mathbf{e}_2 \otimes \mathbf{e}_1) + \mathbf{e}_2 \otimes \mathbf{e}_2 + \mathbf{e}_3 \otimes \mathbf{e}_3. \tag{3.3}$$

The eigenvalues of $\mathbf{B}$ are as follows:

$$\begin{cases} b_1 = (2 + \gamma^2 + \gamma\sqrt{4 + \gamma^2})/2, \\ b_2 = (2 + \gamma^2 - \gamma\sqrt{4 + \gamma^2})/2 = b_1^{-1}, \\ b_3 = 1. \end{cases} \tag{3.4}$$

The volume ratio is given by

$$J = \sqrt{b_1 b_2 b_3} = 1. \tag{3.5}$$

Hencky's logarithmic strain $\ln \mathbf{V}$ is defined as follows:

$$\ln \mathbf{V} = \sum_{\sigma=1}^{m} (\ln \sqrt{b_\sigma})\mathbf{B}_\sigma. \tag{3.6}$$

For simple shear deformation we have (cf. Xiao et al., 1997b)

$$\ln \mathbf{V} = \frac{\ln b_1 - \ln b_2}{2(b_1 - b_2)}(\mathbf{B} - \mathbf{e}_3 \otimes \mathbf{e}_3) + \frac{b_1 \ln b_2 - b_2 \ln b_1}{2(b_1 - b_2)}(\mathbf{I} - \mathbf{e}_3 \otimes \mathbf{e}_3).$$

Hence,

$$\ln \mathbf{V} = \frac{\mathrm{sh}^{-1}\omega}{\sqrt{1+\omega^2}}(\omega(\mathbf{e}_1 \otimes \mathbf{e}_1 - \mathbf{e}_2 \otimes \mathbf{e}_2) + \mathbf{e}_1 \otimes \mathbf{e}_2 + \mathbf{e}_2 \otimes \mathbf{e}_1). \tag{3.7}$$

Here and henceforth

$$\omega = \frac{\gamma}{2}, \tag{3.8}$$

and $\mathrm{sh}^{-1}\omega$ is used to represent the inverse hyperbolic sine function of ω, i.e.

$$\mathrm{sh}^{-1}\omega = \ln(\omega + \sqrt{1+\omega^2}).$$

The stretching $\mathbf{D}$ and the vorticity tensor $\mathbf{W}$ are given by

$$\mathbf{D} = \dot{\omega}(\mathbf{e}_1 \otimes \mathbf{e}_2 + \mathbf{e}_2 \otimes \mathbf{e}_1), \tag{3.9}$$

$$\mathbf{W} = \dot{\omega}(\mathbf{e}_1 \otimes \mathbf{e}_2 - \mathbf{e}_2 \otimes \mathbf{e}_1). \tag{3.10}$$

For the simple shear deformation (3.1), the log-spin $\boldsymbol{\Omega}^{\log}$ is of the form

$$\boldsymbol{\Omega}^{\log} = \frac{1}{2}\dot{\omega}\left(\frac{1}{1+\omega^2} + \frac{\omega}{\sqrt{1+\omega^2}\,\mathrm{sh}^{-1}\omega}\right)(\mathbf{e}_1 \otimes \mathbf{e}_2 - \mathbf{e}_2 \otimes \mathbf{e}_1). \tag{3.11}$$

The process of the simple shear response is simple: the elastic response with $\mathbf{D}^{\mathrm{p}} = \mathbf{0}$ starts at $\omega = 0$ and ends at a yield point $\omega = \omega_0$ and then follows the elastic–plastic response with $\mathbf{D}^{\mathrm{p}} \neq \mathbf{0}$ for all $\omega \geqslant \omega_0$. The two stages will be discussed separately in the succeeding sections.

4. The elastic response and elastic–plastic transition

For the elastic stage, both the elastic–plastic strain rate $\mathbf{D}^{\mathrm{p}}$ and the plastic multiplier $\dot{\rho}$ vanish. Hence, the rate constitutive equations (2.11)–(2.13) are reduced to the hypoelastic equation with the logarithmic stress rate

$$\overset{\circ}{\boldsymbol{\tau}}{}^{\log} = \lambda\,\overline{\dot{\ln J}}\,\mathbf{I} + 2\mu\mathbf{D}. \tag{4.1}$$

It is known that the Eulerian strain rate $\mathbf{D}$ is exactly expressible as the logarithmic rate of Hencky's logarithmic strain measure $\ln \mathbf{V}$ defined by Eq. (3.6), i.e., the rigorous kinematical relation (see, e.g., Xiao et al., 1997a, 1998a,b)

$$\mathbf{D} = \overset{\circ}{\overline{\ln \mathbf{V}}}{}^{\log} \equiv \overline{\dot{\ln \mathbf{V}}} + (\ln \mathbf{V})\boldsymbol{\Omega}^{\log} - \boldsymbol{\Omega}^{\log}(\ln \mathbf{V}) \tag{4.2}$$

holds. Utilizing Eq. (4.2) and the relations (2.18) and (2.19), we deduce that the application of the logarithmic stress rate $\overset{\circ}{\boldsymbol{\tau}}{}^{\log}$ makes the hypoelastic equation (4.1) to be integrable exactly to deliver a finite hyperelastic equation characterized by a linear relationship between the Kirchhoff stress $\boldsymbol{\tau}$ and the Hencky's logarithmic strain measure $\ln \mathbf{V}$, i.e. (see Xiao et al., 1997a,b for detail)

$$\boldsymbol{\tau} = \lambda(\ln J)\mathbf{I} + 2\mu \ln \mathbf{V}. \tag{4.3}$$

The latter is exactly the finite elastic relation discussed and advocated by Anand (1979, 1986). In the comprehensive and convincing study made in the just-mentioned references, it is demonstrated that

Eq. (4.3), and accordingly its equivalent rate form (4.1), should have applicability for a wide class of materials for moderately large deformations. Further properties of Eqs. (4.1) and (4.3) are indicated in Bruhns et al. (2000).

It follows from Eqs. (3.5) and (3.7) that the elastic response is given by

$$\frac{\boldsymbol{\tau}}{2\mu} = \ln \mathbf{V} = \frac{\mathrm{sh}^{-1}\omega}{\sqrt{1+\omega^2}}(\omega(\mathbf{e}_1 \otimes \mathbf{e}_1 - \mathbf{e}_2 \otimes \mathbf{e}_2) + \mathbf{e}_1 \otimes \mathbf{e}_2 + \mathbf{e}_2 \otimes \mathbf{e}_1). \tag{4.4}$$

Thus, we have

$$\frac{\tau_{12}}{2\mu} = \frac{\mathrm{sh}^{-1}\omega}{\sqrt{1+\omega^2}}, \tag{4.5}$$

$$\tau_{11} = -\tau_{22} = \omega\tau_{12}. \tag{4.6}$$

The above elastic response starts at $\omega = 0$ and concludes with the yield condition (2.6) fulfiled, i.e.

$$\tau_{12}^2 + \tau_{11}^2 = \frac{1}{3}\sigma_0^2, \tag{4.7}$$

which corresponds to the yield point $\omega = \omega_0$. Using the expressions (4.5) and (4.6), we infer that ω_0 is determined by

$$\omega_0 = \mathrm{sh}\frac{\sqrt{3}\sigma_0}{6\mu}. \tag{4.8}$$

Throughout, $\mathrm{sh}\omega$ and $\mathrm{ch}\omega$ are used to represent the hyperbolic sine and cosine functions of ω. Let further

$$\tau_{ij}^0 = \tau_{ij}|_{\omega=\omega_0}. \tag{4.9}$$

Then we have the non-vanishing stress components

$$\tau_{12}^0 = \frac{\sigma_0}{\sqrt{3}}\frac{1}{\mathrm{ch}(\sqrt{3}\sigma_0/6\mu)}, \tag{4.10}$$

$$\tau_{11}^0 = -\tau_{22}^0 = \omega_0\tau_{12}^0. \tag{4.11}$$

5. The elastic–plastic response

5.1. The governing equation

During loading, and for $\omega \geqslant \omega_0$, plastic flow occurs governed by the yield condition (2.6) and the rate equations (2.11)–(2.13). Decomposing the stress $\boldsymbol{\tau}$ in the form

$$\boldsymbol{\tau} = \boldsymbol{\alpha} + \boldsymbol{\chi} + \frac{1}{3}(\mathrm{tr}\boldsymbol{\tau})\mathbf{I} \tag{5.1}$$

and utilizing Eqs. (3.5), (3.6) and (3.9), from Eqs. (2.11)–(2.13) we derive the following governing equation for plastic flow:

$$\mathrm{tr}\boldsymbol{\tau} = 0, \tag{5.2}$$

$$\overset{\circ}{\boldsymbol{\chi}}{}^{\log} = 2\mu\mathbf{D} - \frac{4\mu}{\sigma_0^2}(\dot{\omega}\chi_{12})\boldsymbol{\chi}, \tag{5.3}$$

$$\overset{\circ}{\boldsymbol{\alpha}}{}^{\log} = c\left(\mathbf{D} - \frac{1}{2\mu}\overset{\circ}{\boldsymbol{\tau}}{}^{\log}\right). \tag{5.4}$$

The initial conditions for plastic flow are given by Eqs. (4.9)–(4.11) and

$$\boldsymbol{\alpha}|_{\omega=\omega_0} = \mathbf{0}. \tag{5.5}$$

In what follows we shall work out the solution of Eqs. (5.2)–(5.4) with the initial conditions at the elastic–plastic transition.

First, we treat Eq. (5.4) with Eq. (5.5). Utilizing the relations (2.18) and (2.19), we recast Eq. (5.4) in the form

$$\dot{\overline{(\mathbf{R}^{\log} \bigstar \boldsymbol{\alpha})}} = c\dot{\overline{(\mathbf{R}^{\log} \bigstar \ln \mathbf{V})}} - \frac{c}{2\mu}\dot{\overline{(\mathbf{R}^{\log} \bigstar \boldsymbol{\tau})}}.$$

Then, using the initial condition (5.5) we derive

$$(\mathbf{R}^{\log} \bigstar \boldsymbol{\alpha})|_{\omega_0}^{\omega} = c(\mathbf{R}^{\log} \bigstar \ln \mathbf{V})|_{\omega_0}^{\omega} - \frac{c}{2\mu}(\mathbf{R}^{\log} \bigstar \boldsymbol{\tau})|_{\omega_0}^{\omega}$$

for linear hardening, i.e., for a constant c. Hence, by using the latter and $(4.4)_1$ at $\omega = \omega_0$ we obtain

$$\boldsymbol{\alpha} = c\left(\ln \mathbf{V} - \frac{1}{2\mu}\boldsymbol{\tau}\right).$$

Thus, from the latter and Eqs. (5.1) and (3.5) we derive

$$\boldsymbol{\alpha} = \frac{c}{c + 2\mu}(2\mu \ln \mathbf{V} - \boldsymbol{\chi}) \tag{5.6}$$

for $\omega \geqslant \omega_0$. In Eq. (5.6), the logarithmic strain $\ln \mathbf{V}$ is given by Eq. (3.7) and the effective stress $\boldsymbol{\chi}$ (cf. Eq. (2.10)) is determined by Eq. (5.3) and the initial condition at the elastic–plastic transition.

Next, we treat Eq. (5.3) for the effective stress $\boldsymbol{\chi}$. Owing to Eq. (3.5), the Kirchhoff stress $\boldsymbol{\tau}$ is equal to the Cauchy stress $\boldsymbol{\sigma}$ and of the form

$$\boldsymbol{\tau} = \tau_{11}\mathbf{e}_1 \otimes \mathbf{e}_1 + \tau_{22}\mathbf{e}_2 \otimes \mathbf{e}_2 + \tau_{12}(\mathbf{e}_1 \otimes \mathbf{e}_2 + \mathbf{e}_2 \otimes \mathbf{e}_1) - (\tau_{11} + \tau_{22})\mathbf{e}_3 \otimes \mathbf{e}_3.$$

The back stress $\boldsymbol{\alpha}$ and therefore the effective stress $\boldsymbol{\chi}$ are of the same form. Substituting the above form and Eqs. (3.9) and (3.11) into Eq. (5.3) and using $\dot{\chi}_{ij} = \dot{\omega}(\mathrm{d}\chi_{ij}/\mathrm{d}\omega)$, for $\omega \geqslant \omega_0$ we obtain the coupled system of differential equations

$$\frac{\mathrm{d}\chi_{11}}{\mathrm{d}\omega} - g(\omega)\chi_{12} = -\frac{6\mu}{\sigma_0^2}\chi_{12}\chi_{11}, \tag{5.7}$$

$$\frac{\mathrm{d}\chi_{22}}{\mathrm{d}\omega} + g(\omega)\chi_{12} = -\frac{6\mu}{\sigma_0^2}\chi_{12}\chi_{22}, \tag{5.8}$$

$$\frac{\mathrm{d}\chi_{12}}{\mathrm{d}\omega} + \frac{1}{2}g(\omega)(\chi_{11} - \chi_{22}) = 2\mu - \frac{6\mu}{\sigma_0^2}\chi_{12}^2, \tag{5.9}$$

$$-\frac{\mathrm{d}(\chi_{11} + \chi_{22})}{\mathrm{d}\omega} = \frac{6\mu}{\sigma_0^2}\chi_{12}(\chi_{11} + \chi_{22}), \tag{5.10}$$

with the following initial conditions (cf. Eqs. (4.10), (4.11) and (5.5)) at the elastic–plastic transition

$$\chi_{ij}|_{\omega=\omega_0} = \tau_{ij}^0, \quad ij = 11, 22, 12. \tag{5.11}$$

In Eqs. (5.7)–(5.9), we have introduced

$$g(\omega) = \frac{1}{1+\omega^2} + \frac{\omega}{\sqrt{1+\omega^2}\,\mathrm{sh}^{-1}\omega}. \tag{5.12}$$

From Eq. (5.10) and the initial value $\chi_{11}^0 + \chi_{22}^0 = 0$, we deduce

$$\chi_{11} + \chi_{22} = 0, \quad \text{i.e.} \quad \chi_{22} = -\chi_{11}. \tag{5.13}$$

Incorporating the above facts, from Eqs. (5.7)–(5.10), (4.10) and the yield condition (4.7) we derive a single governing equation for the effective stress $\boldsymbol{\chi}$ as follows:

$$\frac{\mathrm{d}\chi_{12}}{\mathrm{d}\omega} + g(\omega)\sqrt{\frac{1}{3}\sigma_0^2 - \chi_{12}^2} = 2\mu - \frac{6\mu}{\sigma_0^2}\chi_{12}^2 \tag{5.14}$$

with the initial condition

$$\chi_{12}|_{\omega=\omega_0} = \tau_{12}^0 = \frac{\sigma_0}{\sqrt{3}}\left(\mathrm{ch}\frac{\sqrt{3}\sigma_0}{6\mu}\right)^{-1}. \tag{5.15}$$

Once the shear component χ_{12} is known, the other non-vanishing components are obtained by

$$\chi_{11} = -\chi_{22} = \sqrt{\frac{1}{3}\sigma_0^2 - \chi_{12}^2}. \tag{5.16}$$

5.2. A singular perturbation solution

It seems to be not easy to derive a closed-form solution for the nonlinear ordinary differential equation (5.14) with the prescribed initial condition (5.15). In fact, with the transformation

$$\chi_{12} = \frac{\sigma_0}{\sqrt{3}}\cos\theta, \tag{5.17}$$

and accordingly (cf. Eq. (5.16))

$$\chi_{11} = -\chi_{22} = \frac{\sigma_0}{\sqrt{3}}\sin\theta, \tag{5.18}$$

Eq. (5.14) with Eq. (5.15) is recast in the form

$$\frac{\mathrm{d}\theta}{\mathrm{d}\omega} + (2\sqrt{3}\mu\sigma_0^{-1})\sin\theta = g(\omega) \tag{5.19}$$

with

$$\theta|_{\omega=\omega_0} = \cos^{-1}\left\{\left(\mathrm{ch}\frac{\sqrt{3}\sigma_0}{6\mu}\right)^{-1}\right\}. \tag{5.20}$$

A further transformation can show that Eq. (5.19) is a Riccati equation for which no closed-form solution can be derived. However, the elastic shear modulus μ is usually much greater than the tensile yield strength σ_0 for metals and alloys etc. This suggests that an approximate analytical solution for the problem at issue may be obtainable. Indeed, introducing the dimensionless material parameter

$$\epsilon = \frac{\sqrt{3}\sigma_0}{6\mu}, \tag{5.21}$$

Eq. (5.19) may be reformulated as

$$\epsilon\frac{\mathrm{d}\theta}{\mathrm{d}\omega}+\sin\theta=\epsilon g(\omega) \tag{5.22}$$

$$\theta|_{\omega=\mathrm{sh}\epsilon}=\cos^{-1}\left(\frac{1}{\mathrm{ch}\epsilon}\right). \tag{5.23}$$

The order of magnitude of the dimensionless material parameter ϵ usually falls within 10^{-2}–10^{-4}. Thus, it becomes clear that Eq. (5.22) is a first-order ordinary differential equation of singular type with a small parameter ϵ multiplying the highest derivative. Moreover, the small parameter ϵ is also involved in the initial condition (5.23).

We may introduce a small interval, called *boundary layer*, at the point $\omega=\omega_0=\mathrm{sh}\epsilon$. The exact solution of Eq. (5.22) changes very quickly within this layer and normally beyond it. We shall apply the method of matched expansions (see, e.g., Nayfeh, 1973) to derive a singular perturbation solution for Eq. (5.22). According to this method, an outer solution θ^{o}, which applies beyond the boundary layer, and an inner solution θ^{i}, which is valid within the boundary layer, are determined separately, and then a composite solution is formed by a matching procedure. This will be done as follows:

First, we express the outer solution θ^{o} as the asymptotic expression

$$\theta^{\mathrm{o}}=\theta_0^{\mathrm{o}}+\epsilon\theta_1^{\mathrm{o}}+\cdots.$$

Then, substituting it into Eq. (5.22) and expanding all functions involved as Taylor's series in terms of ϵ, we derive

$$\sin\theta_0^{\mathrm{o}}=0,\quad \theta_1^{\mathrm{o}}=g(\omega),$$

etc. Hence, we have

$$\theta^{\mathrm{o}}=\epsilon g(\omega)+O(\epsilon^2). \tag{5.24}$$

Evidently, the above solution does not satisfy the initial condition (5.23). This issue will be treated below at $\omega_0=\mathrm{sh}\epsilon$ by considering the inner solution θ^{i}.

Second, in order to determine the inner solution θ^{i}, we magnify the boundary layer by using the stretching transformation

$$\bar{\omega}=\frac{\omega-\mathrm{sh}\epsilon}{\epsilon}. \tag{5.25}$$

With this transformation, Eqs. (5.22) and (5.23) become

$$\frac{\mathrm{d}\theta^{\mathrm{i}}}{\mathrm{d}\bar{\omega}}+\sin\theta^{\mathrm{i}}=\epsilon g(\epsilon\bar{\omega}+\mathrm{sh}\epsilon) \tag{5.26}$$

with

$$\theta^{\mathrm{i}}|_{\bar{\omega}=0}=\sin^{-1}\left(\frac{\mathrm{sh}\epsilon}{\mathrm{ch}\epsilon}\right). \tag{5.27}$$

In deriving the latter, the identity $\cos^{-1}x=\sin^{-1}\sqrt{1-x^2}$ is used. Then, substituting the asymptotic expansion

$$\theta^{\mathrm{i}}=\theta_0^{\mathrm{i}}(\bar{\omega})+\epsilon\theta_1^{\mathrm{i}}(\bar{\omega})+\cdots$$

into Eqs. (5.26) and (5.27), utilizing different Taylor's expansions

$$g(\epsilon\bar{\omega}+\mathrm{sh}\epsilon)=2+\tfrac{1}{2}\epsilon^2 g''(0)(1+\bar{\omega})^2+\cdots$$

and then equating the coefficients of ϵ^s for all s to zero, we derive perturbation equations for $\theta^{\mathrm{i}}_s = \theta^{\mathrm{i}}_s(\bar{\omega})$. The first two equations for $s = 0$, 1 are

$$\frac{\mathrm{d}\theta^{\mathrm{i}}_0}{\mathrm{d}\bar{\omega}} + \sin\theta^{\mathrm{i}}_0 = 0, \quad \theta^{\mathrm{i}}_0|_{\bar{\omega}=0} = 0,$$

$$\frac{\mathrm{d}\theta^{\mathrm{i}}_1}{\mathrm{d}\bar{\omega}} + \theta^{\mathrm{i}}_1 \cos\theta^{\mathrm{i}}_0 = 2, \quad \theta^{\mathrm{i}}_1|_{\bar{\omega}=0} = 1.$$

Hence, we have

$$\theta^{\mathrm{i}} = \epsilon(2 - \exp(-\bar{\omega})) + O(\epsilon^2). \tag{5.28}$$

Third, we consider the following matching condition for the outer and inner solutions θ^{o} and θ^{i}:

$$\lim_{\bar{\omega}\to+\infty} \theta^{\mathrm{i}}(\bar{\omega}) = \lim_{\omega\to+\mathrm{sh}\epsilon} \theta^{\mathrm{o}}(\omega) = \text{constant} = a.$$

It may readily be shown that the above condition is satisfied and

$$a = 2\epsilon.$$

Thus, the composite solution is given by

$$\theta = \theta^{\mathrm{o}} + \theta^{\mathrm{i}} - a = \epsilon(g(\omega) - \exp(-\bar{\omega})) + O(\epsilon^2). \tag{5.29}$$

From the latter and Eqs. (5.12), (5.17) and (5.18) we obtain the following solutions for the nonvanishing components of the effective stress $\boldsymbol{\chi}$:

$$\chi_{12} = \frac{\sigma_0}{\sqrt{3}}\left(1 - \frac{1}{2}\epsilon^2(g(\omega) - \exp(-\bar{\omega}))^2\right) + O(\epsilon^3), \tag{5.30}$$

$$\chi_{11} = -\chi_{22} = \frac{\sigma_0}{\sqrt{3}}\epsilon(g(\omega) - \exp(-\bar{\omega})) + O(\epsilon^3). \tag{5.31}$$

From the above solutions and Eqs. (5.6) and (3.7), we can obtain the different components of the back stress α, and finally we arrive at the nonvanishing stress components

$$\tau_{12} = \frac{2\mu}{c + 2\mu}\left\{\frac{\sigma_0}{\sqrt{3}}\left(1 - \frac{1}{2}\epsilon^2(g(\omega) - \exp(-\bar{\omega}))^2\right) + c\frac{\mathrm{sh}^{-1}\omega}{\sqrt{1+\omega^2}}\right\} + O(\epsilon^3), \tag{5.32}$$

$$\tau_{11} = -\tau_{22} = \frac{2\mu}{c + 2\mu}\left\{\frac{\sigma_0}{\sqrt{3}}\epsilon(g(\omega) - \exp(-\bar{\omega})) + c\frac{\omega\mathrm{sh}^{-1}\omega}{\sqrt{1+\omega^2}}\right\} + O(\epsilon^3). \tag{5.33}$$

6. Analysis: the coupling effect of material properties

The stress-deformation responses, i.e. here, the τ_{12}–ω and τ_{11}–ω curves, are characterized by the coupling of elastic, yielding and hardening properties. This coupling effect may be studied for general material parameters μ, σ_0 and c by analyzing the analytical solutions (5.32) and (5.33). Towards this goal, we evaluate the derivatives of the plastic solutions (5.32) and (5.33), which are given by

$$\frac{1}{\beta}\frac{\mathrm{d}\tau_{12}}{\mathrm{d}\omega} = c\left(\frac{1}{1+\omega^2} - \frac{\omega\mathrm{sh}^{-1}\omega}{(1+\omega^2)^{1.5}}\right) - \frac{\sigma_0}{\sqrt{3}}\epsilon^2(g(\omega) - \exp(-\bar{\omega}))(g'(\omega) + \epsilon^{-1}\exp(-\bar{\omega})), \tag{6.1}$$

$$\frac{1}{\beta}\frac{\mathrm{d}\tau_{11}}{\mathrm{d}\omega} = c\left(\frac{\omega}{1+\omega^2} + \frac{\mathrm{sh}^{-1}\omega}{(1+\omega^2)^{1.5}}\right) + \frac{\sigma_0}{\sqrt{3}}\epsilon(g'(\omega) + \epsilon^{-1}\exp(-\bar{\omega})), \tag{6.2}$$

where $\beta = 2\mu/(c+2\mu)$ and

$$g'(\omega) = \frac{\mathrm{d}g}{\mathrm{d}\omega} = \frac{1}{(1+\omega^2)^{1.5}\mathrm{sh}^{-1}\omega} - \frac{\omega}{1+\omega^2}\left(\frac{2}{1+\omega^2} + \frac{1}{(\mathrm{sh}^{-1}\omega)^2}\right), \tag{6.3}$$

and $\bar{\omega}$ and $g(\omega)$ are given by Eqs. (5.12) and (5.25).

Given the elastic shear modulus 2μ, the initial yield stress σ_0 and the hardening modulus c, we need to know how the stresses τ_{12} and τ_{11}, respectively, change with the increasing shear strain ω. This can be done by judging the sign of the derivatives given above. Several cases will be discussed below.

6.1. Elastic-perfect plasticity

In this case we have $c = 0$ and thus Eqs. (5.32) and (5.33) yield

$$\tau_{12} = \frac{\sigma_0}{\sqrt{3}}\left(1 - \frac{1}{2}\epsilon^2(g(\omega) - \exp(-\bar{\omega}))^2\right), \tag{6.4}$$

$$\tau_{11} = -\tau_{22} = \frac{\sigma_0}{\sqrt{3}}\epsilon(g(\omega) - \exp(-\bar{\omega})), \tag{6.5}$$

and Eqs. (6.1) and (6.2) produce

$$\frac{\mathrm{d}\tau_{12}}{\mathrm{d}\omega} = -\frac{\sigma_0}{\sqrt{3}}\epsilon^2(g(\omega) - \exp(-\bar{\omega}))(g'(\omega) + \epsilon^{-1}\exp(-\bar{\omega})), \tag{6.6}$$

$$\frac{d\tau_{11}}{d\omega} = \frac{\sigma_0}{\sqrt{3}}\epsilon(g'(\omega) + \epsilon^{-1}\exp(-\bar{\omega})). \tag{6.7}$$

It can be proved that

$$g(\omega) - \exp(-\bar{\omega}) > 0, \quad \omega > \omega_0. \tag{6.8}$$

Moreover, there is one and only one root $\omega = \omega_{pp}^m > \omega_0$ satisfying the equation

$$g'(\omega) + \epsilon^{-1}\exp(-\bar{\omega}) = 0. \tag{6.9}$$

The unique root $\omega_{pp}^m > \omega_0$ is close to ϵ and of the same order of magnitude as $-\epsilon\ln\epsilon$, i.e. (for $\sigma_0/2\mu = 0.05$)

$$\omega_{pp}^m = 0.1576.$$

We have

$$\begin{cases} \frac{\mathrm{d}\tau_{12}}{\mathrm{d}\omega} < 0 \text{ and } \frac{\mathrm{d}\tau_{11}}{\mathrm{d}\omega} > 0 & \text{for } \omega_0 < \omega < \omega_{pp}^m, \\ \frac{\mathrm{d}\tau_{12}}{\mathrm{d}\omega} > 0 \text{ and } \frac{\mathrm{d}\tau_{11}}{\mathrm{d}\omega} < 0 & \text{for } \omega > \omega_{pp}^m. \end{cases} \tag{6.10}$$

Thus, starting with the initial yielding the shear stress τ_{12} (resp., the normal stress τ_{11}) drops (grows) to a minimum (maximum) at ω_{pp}^m and after that slowly grows (drops) to the rigid-plastic value $\sigma_0/\sqrt{3}$ (resp., 0). These properties are shown in Figs. 1 and 2, wherein as an estimate for a theoretical upper limit we have introduced

$$\frac{\sigma_0}{2\mu} = 0.05.$$

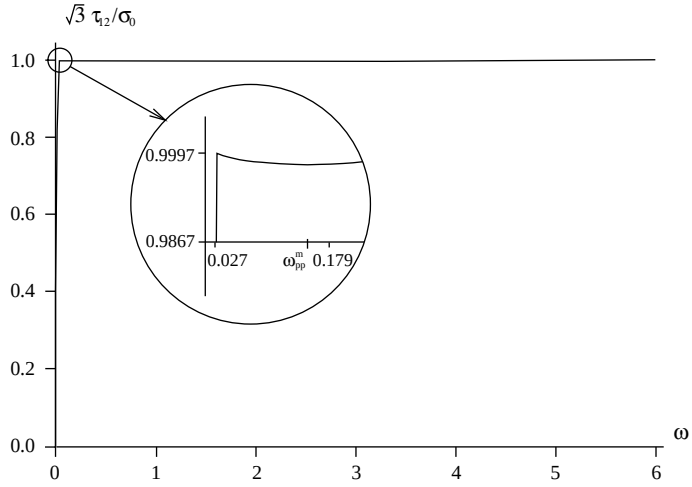

Fig. 1. Elastic-perfect plasticity: normalized shear stress vs shear strain ω.

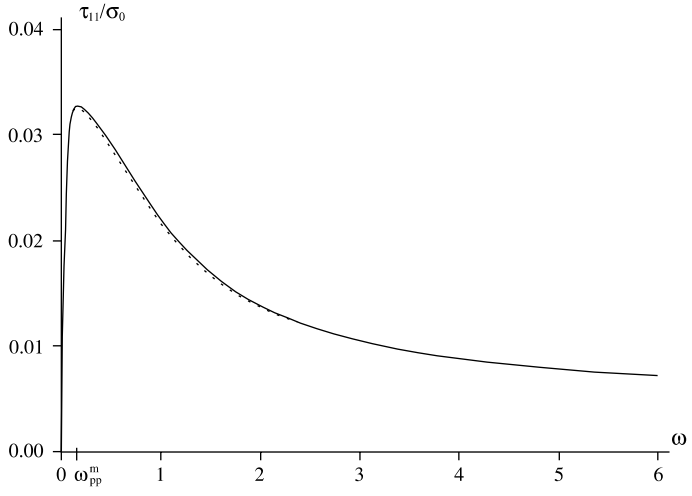

Fig. 2. Elastic-perfect plasticity: normalized axial stress vs shear strain ω.

In these figures the full lines describe the Runge–Kutta solution of the original system (Eqs. (5.14)–(5.16)), whereas the closed-form expressions for the shear stress τ_{12} and the normal stress τ_{11} according to Eqs. (6.4) and (6.5) are given with dotted lines. It turned out that the exact solutions and the perturbation solutions are almost identical – even for the extremely high value of σ_0 under consideration. In Fig. 1, where the shear stress τ_{12} is indicated, both solutions coincide within the accuracy of our presentation. The magnification of Fig. 2 (and Fig. 8, given later) is needed to discover however, a small deviation of both solutions. Therefore it seems to be admissible that the analytical perturbation solution can be taken as solution of the underlying simple shear and torsion problems.

The above analysis also shows that within the boundary layer $(\omega_0, \omega_{pp}^m)$ appears a slight instability immediately following initial yielding. This phenomenon was observed by Moss (1984) and later further

discussed in detail by Tsakmakis and Haupt (1989). It may be expected that a similar phenomenon will occur whenever the hardening is weak enough. This will be discussed later.

6.2. Kinematic hardening rigid plasticity

In this case the shear modulus $\mu \to \infty$, and consequently Eqs. (5.32) and (5.33) collapse to

$$\tau_{12} = \frac{\sigma_0}{\sqrt{3}} + c\frac{\mathrm{sh}^{-1}\omega}{\sqrt{1+\omega^2}}, \tag{6.11}$$

$$\tau_{11} = -\tau_{22} = c\frac{\omega \mathrm{sh}^{-1}\omega}{\sqrt{1+\omega^2}}, \tag{6.12}$$

and Eqs. (6.1) and (6.2) to

$$\frac{\mathrm{d}\tau_{12}}{\mathrm{d}\omega} = c\left(\frac{1}{1+\omega^2} - \frac{\omega \mathrm{sh}^{-1}\omega}{(1+\omega^2)^{1.5}}\right), \tag{6.13}$$

$$\frac{\mathrm{d}\tau_{11}}{\mathrm{d}\omega} = c\left(\frac{\omega}{1+\omega^2} + \frac{\mathrm{sh}^{-1}\omega}{(1+\omega^2)^{1.5}}\right), \tag{6.14}$$

The former has one and only one zero point $\omega = \omega_{kp}^m$, determined by

$$\sqrt{1+\omega^2} - \omega \ln\left(\omega + \sqrt{1+\omega^2}\right) = 0, \tag{6.15}$$

i.e.,

$$\omega_{kp}^m = 1.5088. \tag{6.16}$$

We have

$$\frac{\mathrm{d}\tau_{12}}{\mathrm{d}\omega} > 0 \quad \text{for } \omega_0 < \omega < \omega_{kp}^m \quad \text{and} \quad \frac{\mathrm{d}\tau_{12}}{\mathrm{d}\omega} < 0 \quad \text{for } \omega > \omega_{kp}^m, \tag{6.17}$$

and evidently,

$$\frac{\mathrm{d}\tau_{11}}{\mathrm{d}\omega} > 0 \quad \text{for } \omega > \omega_0. \tag{6.18}$$

Thus, the normal stress τ_{11} invariably grows with increasing shear strain $\omega > \omega_0$. Starting with its initial yield value $\sigma_0/\sqrt{3}$ the shear stress τ_{12} grows to its upper bound τ_{12}^m at ω_{kp}^m and after that drops back as a limit to its initial yield value $\sigma_0/\sqrt{3}$ with ω growing unlimited. The upper bound, i.e., the shear strength, is given by

$$\tau_{12}^m = \frac{\sigma_0}{\sqrt{3}}\left(1 + \frac{\sqrt{3}}{\omega_{kp}^m}\frac{c}{\sigma_0}\right) \doteq 0.5773\sigma_0 + 0.6627c. \tag{6.19}$$

The normalized shear stress–shear strain and axial stress–shear strain curves are shown in Figs. 3 and 4. As before the exact solution and the perturbation solution agree extremely well.

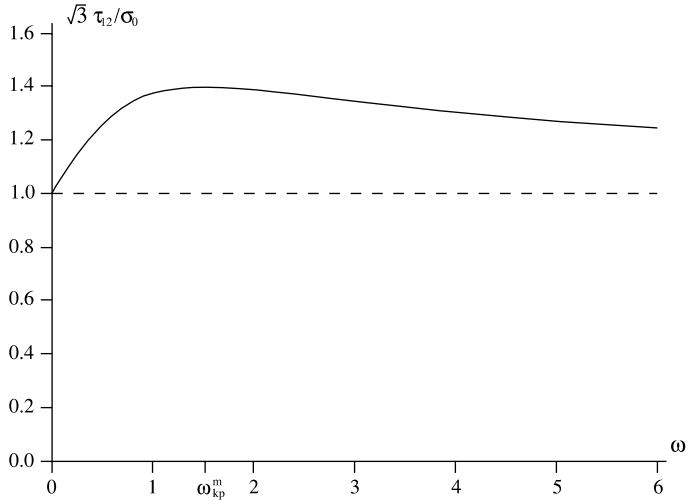

Fig. 3. Kinematic hardening plasticity: normalized shear stress vs shear strain ω, with normalized hardening parameter $\sqrt{3}c/\sigma_0 = 0.6$.

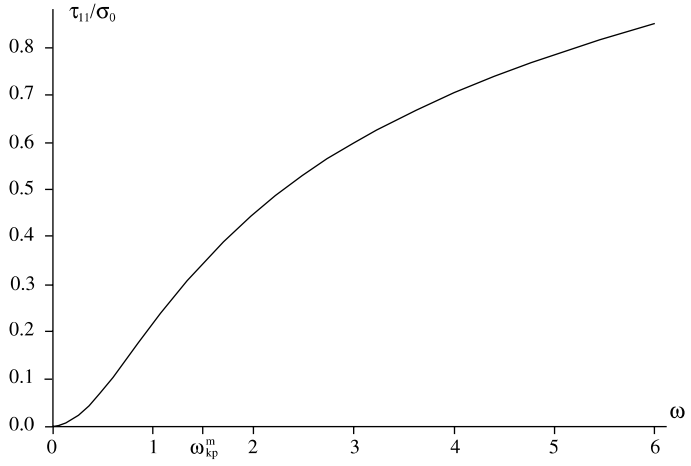

Fig. 4. Kinematic hardening plasticity: normalized axial stress vs shear strain ω, with normalized hardening parameter $\sqrt{3}c/\sigma_0 = 0.6$.

6.3. Kinematic hardening elasto-plasticity

In this general case, both the τ_{12}–ω and τ_{11}–ω curves will manifest themselves in a more complicated manner due to the coupling effect of elastic, yielding and hardening properties. In what follows, a detailed analysis of this coupling will be made. Towards this goal, we evaluate the derivatives given by Eqs. (6.1) and (6.2).

First, we consider the shear stress τ_{12}. When ω falls within the boundary layer $(\omega_0, \omega_{pp}^m)$, the first term of Eq. (6.1) is positive and the second negative. In this case, the sign of the derivative (6.1) depends on whether the hardening is weak or strong. We have

$$\left.\frac{\mathrm{d}\tau_{12}}{\mathrm{d}\omega}\right|_{\omega=\omega_0} = \beta\left(c - \frac{\sigma_0}{\sqrt{3}}\epsilon\right) + O(\epsilon^2), \quad \left.\frac{\mathrm{d}\tau_{12}}{\mathrm{d}\omega}\right|_{\omega=\omega_{pp}^m} > 0.$$

Then, it may be proved that, within the foregoing boundary layer, the derivative $\mathrm{d}\tau_{12}/\mathrm{d}\omega$ has one and only one zero point ω_{k0}^m, whenever $\sqrt{3}c/\sigma_0 - \epsilon < 0$, i.e.,

$$c < \frac{\sigma_0^2}{6\mu}, \tag{6.20}$$

whereas the derivative $\mathrm{d}\tau_{12}/\mathrm{d}\omega$ is positive and has no zero point, whenever

$$c \geqslant \frac{\sigma_0^2}{6\mu}. \tag{6.21}$$

On the other hand, when ω leaves the boundary layer, the exponential function $\exp(-\bar{\omega})$ more rapidly approaches zero than any ϵ^r with $r > 0$ and hence may be negligible. In this case, the zero points of the derivative $\mathrm{d}\tau_{12}/\mathrm{d}\omega$ are determined by

$$\sqrt{3}\frac{c}{\sigma_0}\left(\sqrt{1+\omega^2} - \omega \ln\left(\omega + \sqrt{1+\omega^2}\right)\right) = \epsilon^2 g(\omega) g'(\omega)(1+\omega^2)^{1.5}. \tag{6.22}$$

It can be proved that Eq. (6.22) has one and only one root, ω_{k1}^m, for any given material parameters $\epsilon \geqslant 0$ and $c > 0$. Usually, ϵ^2 is much smaller than $\sqrt{3}c/\sigma_0$. As a result, this unique root ω_{k1}^m is very close to ω_{kp}^m.

Combining the above discussion, we describe the property of the τ_{12}–ω curve as follows. If the hardening is weak as indicated by Eq. (6.20), then, immediately following the initial yielding over a very thin layer $(\omega_0, \omega_{k0}^m)$ the shear stress τ_{12} drops to a value slightly smaller than its initial yield value, after that grows to its maximum at $\omega = \omega_{k1}^m$, and finally drops to as a limit the rigid plastic value $\sigma_0/\sqrt{3}$. This is shown in Fig. 5, where here we have introduced

$$\frac{\sqrt{3}c}{\sigma_0} = 0.022.$$

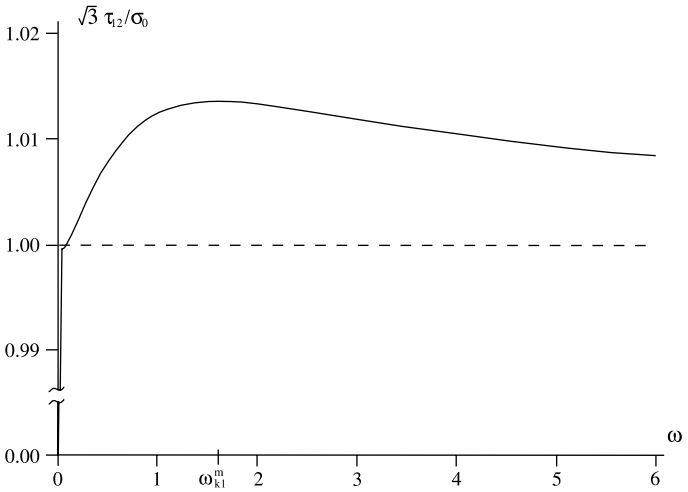

Fig. 5. Coupling effect with Eq. (6.20): normalized shear stress vs shear strain ω, with normalized hardening parameter $\sqrt{3}c/\sigma_0 = 0.022$ and the zero point $\omega_{k1}^m = 1.5931$ from Eq. (6.22). The dashed line marks the value of normalized shear stress τ_{12} at the limit for infinite strain ω.

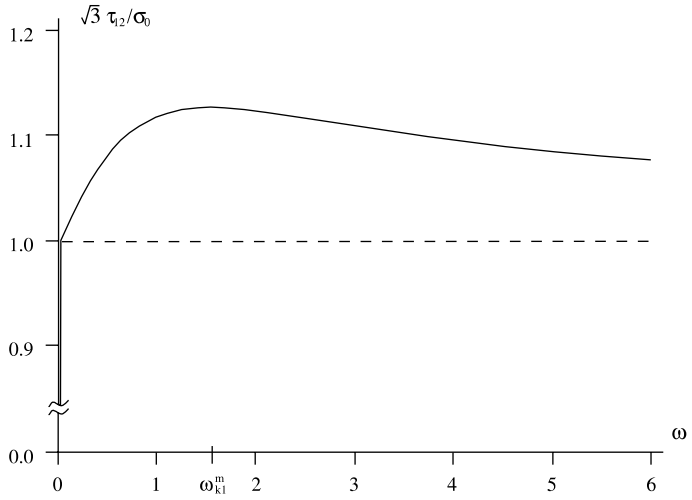

Fig. 6. Coupling effect with Eq. (6.21): normalized shear stress vs shear strain ω, with normalized hardening parameter $\sqrt{3}c/\sigma_0 = 0.2$ and the zero point $\omega_{k1}^m = 1.5183$ from Eq. (6.22). The dashed line marks the value of normalized shear stress τ_{12} at the limit for infinite strain ω.

If the hardening is strong enough to satisfy Eq. (6.21), then starting from the initial yielding the τ_{12}–ω curve will manifest itself in the same manner as in the case of kinematic hardening rigid plasticity, except for the fact that the maximum point ω_{kp}^m of the latter is replaced by a slightly greater one, i.e., ω_{k1}^m. This is shown in Fig. 6, with

$$\frac{\sqrt{3}c}{\sigma_0} = 0.2.$$

From the above, the kinematic hardening elasto-plasticity model with logarithmic rate predicts that, when the increasing shear strain ω arrives at a critical point ω_{k1}^m determined by Eq. (6.22), which is very close to ω_{kp}^m, the shear stress τ_{12} attains its maximum τ_{12}^m and after that instability phenomena may occur. It is noticed that this prediction is in agreement with experimental results reported by, e.g., Billington (1976). In the just-mentioned reference, the reported shear strains ω_{k1}^m at which instability occurs are about 1.4, 1.3 and 1.5, respectively, for thin-walled specimens of aluminum alloy, copper and iron.

Now we consider the axial (normal) stress τ_{11}. Since the inequality (6.18) with Eq. (6.14) holds, the derivative $\mathrm{d}\tau_{11}/\mathrm{d}\omega$ given by Eq. (6.2) has the same sign as the function

$$F(\omega) = \frac{6\mu c}{\sigma_0^2} + \frac{\psi(\omega)}{\phi(\omega)} \tag{6.23}$$

with

$$\psi(\omega) = g'(\omega) + \epsilon^{-1}\exp(-\bar{\omega}), \quad \phi(\omega) = \frac{\omega}{1+\omega^2} + \frac{\mathrm{sh}^{-1}\omega}{(1+\omega^2)^{1.5}}. \tag{6.24}$$

The possible zero point of the derivative $F'(\omega)$ is determined by the equation

$$\psi'(\omega_i)\phi(\omega_i) - \psi(\omega_i)\phi'(\omega_i) = 0. \tag{6.25}$$

It may be proved that there is one and only one zero point ω_i satisfying the above equation for a small $\epsilon > 0$, and that at this unique zero point the function $F(\omega)$ attains its minimum

$$F(\omega_i) = \frac{6\mu c}{\sigma_0^2} + \frac{\psi(\omega_i)}{\phi(\omega_i)}. \tag{6.26}$$

Thus, it becomes clear that the derivative $\mathrm{d}\tau_{11}/\mathrm{d}\omega$ is nonnegative, whenever $F(\omega_i) \geqslant 0$, i.e.,

$$c \geqslant -\frac{\sigma_0^2}{6\mu}\frac{\psi(\omega_i)}{\phi(\omega_i)}, \tag{6.27}$$

whereas the derivative $\mathrm{d}\tau_{11}/\mathrm{d}\omega$ has one local maximum point ω_1^m and one local minimum point ω_2^m determined by

$$\frac{\psi(\omega)}{\phi(\omega)} = -\frac{6\mu c}{\sigma_0^2}, \tag{6.28}$$

whenever $F(\omega_i) < 0$, i.e.,

$$c < -\frac{\sigma_0^2}{6\mu}\frac{\psi(\omega_i)}{\phi(\omega_i)}. \tag{6.29}$$

Combining this discussion, we describe the property of the τ_{11}–ω curve as follows. If the hardening is strong enough to satisfy Eq. (6.27), then the normal (axial) stress τ_{11} grows invariably with increasing shear strain. If the hardening is not so strong, as indicated by Eq. (6.29), then the stress τ_{11} grows to a local maximum at ω_1^m, after that drops to a local minimum at ω_2^m, and finally slowly grows to infinity with the shear strain growing to infinity. In the latter case, the two turning points ω_1^m and ω_2^m are determined from Eq. (6.28). These properties are shown in Figs. 7 and 8, where the different normalized hardening parameters are the same as before, 0.2 in Fig. 7 and 0.022 in Fig. 8, respectively.

Again, both solutions agree extremely well, which can be seen from Fig. 8, where the dotted line gives the τ_{11}–ω curve from the perturbation solution.

Experimental axial stress–shear strain curves have been reported by Montheillet et al. (1984) for Al at room temperature (20°C) and a strain rate of 0.007 s^{-1} and at other cases. It may be seen that the theoretical curve shown in Fig. 8 is qualitatively in a good agreement with the just-mentioned experimental curves. Quantitative simulation may be achieved by choosing suitable material constants. It should be

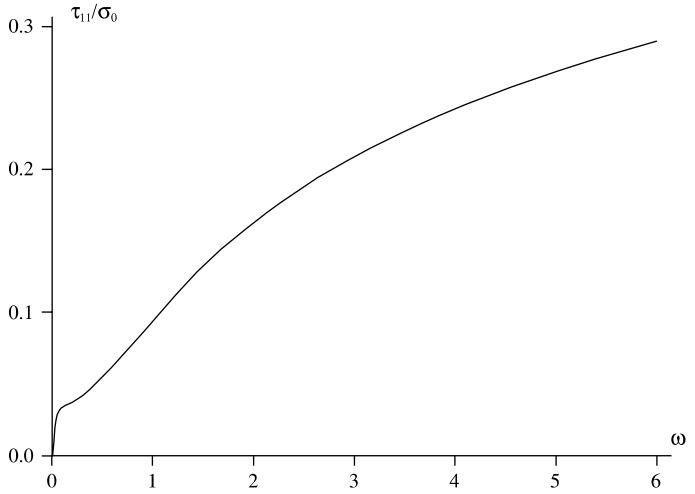

Fig. 7. Coupling effect with Eq. (6.27): normalized axial stress vs shear strain ω, with normalized hardening parameter $\sqrt{3}c/\sigma_0 = 0.2$.

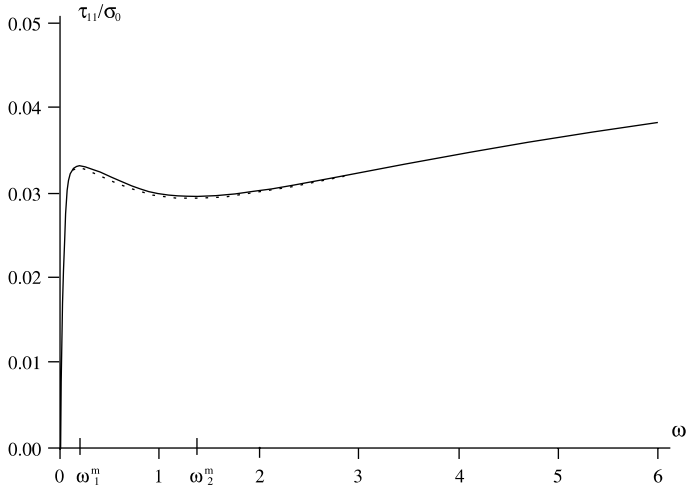

Fig. 8. Coupling effect with Eq. (6.29): normalized axial stress vs shear strain ω, with normalized hardening parameter $\sqrt{3}c/\sigma_0 = 0.022$ and extreme points ω_1^m and ω_2^m from Eq. (6.28).

pointed out that comprehensive simulations of experimental results were successfully made by Ning and Aifantis (1994a) and Cho and Dafalias (1996) and others, by utilizing models with multiple plastic spins and internal variables. The latter usually incorporate a large number of non-classical material parameters. The simple model considered here uses essentially nothing but commonly known classical material constants, i.e., the shear modulus μ, the initial tensile yield stress σ_0 and the hardening modulus c.

7. Discussion

In the previous sections, the kinematic hardening J_2-flow model with the logarithmic tensor rate, proposed in Bruhns et al. (1999), is applied to study the large simple shear and torsional deformation behaviour in elastoplastic bodies such as metals etc. One of the main features of this model as consequence of the logarithmic rate involved is the direct integrability of parts of the constitutive (differential) equations. Combined with a singular perturbation solution analytical forms are obtained which turned out to be almost identical with the exact results from a Runge–Kutta integration. This allows a detailed study of the meaning and coupling effects of the different material properties. For the deformation modes at issue, it is shown that the simple model proposed, which essentially uses nothing but the three classical material constants, i.e., the shear modulus μ, the initial tensile yield stress σ_0 and the hardening modulus c, may supply satisfactory explanations for salient features of complex behaviour observed in experiment. This may suggest the utility and efficacy of the logarithmic tensor rate. In fact, similar models with other objective tensor rates could not arrive at satisfactory explanations for experimental observation, as pointed out by Reed and Atluri (1985).

There are several possibilities to generalize a simple model of the kind at issue. These include the introduction of a general (possibly anisotropic) yield function, extension of the flow rule and development of Prager's kinematic hardening law, as well as incorporation of isotropic hardening, etc. The recent models with an evolving anisotropic flow rule or an anisotropic yield surface or multiple plastic spins etc., proposed in Majors and Krempl (1994), Ning and Aifantis (1994a,b), Cho and Dafalias (1996), Dafalias (2000), Kuroda (1997, 1999), and Kuroda and Tvergaard (2000), are more general and able to simulate in a

comprehensive manner complex behaviour such as axial effect during reversal of torsion, etc. Usually, a more general model may incorporate more material parameters. Their physical explanation and identification requires further investigation in both experimental and micromechanical aspects.

In order to approach more practical problems the logarithmic rate actually is implemented into a finite element code. This implementation will include generalizations like those cited in the foregoing paragraph.

Acknowledgements

This research was completed under the financial support from the Deutsche Forschungsgemeinschaft (DFG) (contract no.: Br 580/26-1). The authors wish to express their sincere gratitude to this support.

References

Agah-Tehrani, A., Lee, E.H., Mallett, R.L., Onat, E.T., 1987. The theory of elastic–plastic deformation at finite strain with induced anisotropy modeled as combined isotropic-kinematical hardening. J. Mech. Phys. Solids 35, 519–539.

Anand, L., 1979. On Hencky's approximate strain-energy function for moderate deformations. J. Appl. Mech. 46, 78–82.

Anand, L., 1986. Moderate deformations in extension-torsion of incompressible isotropic elastic materials. J. Mech. Phys. Solids 34, 293–304.

Atluri, S.N., 1984. On constitutive relations at finite strain: hypo-elasticity and elasto-plasticity with isotropic or kinematic hardening. Comp. Meth. Appl. Mech. Engng. 43, 137–171.

Billington, E.W., 1976. Non-linear mechanical response of various metals: II Permanent length changes in twisted tubes. J. Phys. D: Appl. Phys. 9, 533–552.

Bruhns, O.T., 1973. On the descriptions of cyclic deformation processes using a more general elastoplastic constitutive law. Arch. Mech. 25, 535.

Bruhns, O.T., Xiao, H., Meyers, A., 1999. Self-consistent Eulerian rate type elasto-plasticity model based upon the logarithmic stress rate. Int. J. Plasticity 15, 479–520.

Bruhns, O.T., Xiao, H., Meyers, A., 2000. Hencky's elasticity model with the logarithmic strain: a study on Poynting effect and stress response in torsion of tubes and rods. Arch. Mech. 52, 489–509.

Cho, H.W., Dafalias, Y.F., 1996. Distortional and orientational hardening at large viscoplastic deformations. Int. J. Plasticity 12, 903–925.

Dafalias, Y.F., 1983. Corotational rates for kinematic hardening at large plastic deformations. J. Appl. Mech. 50, 561–565.

Dafalias, Y.F., 2000. Orientational evolution of plastic orthotropy in sheet metals. J. Mech. Phys. Solids 48, 2231–2255.

Dienes, J.K., 1979. On the analysis of rotation and stress rate in deforming bodies. Acta Mechanica 32, 217–232.

Haupt, P., Tsakmakis, Ch., 1986. On kinematic hardening and large plastic deformations. Int. J. Plasticity 2, 279–293.

Johnson, J.C., Bammann, D.J., 1984. A discussion of stress rates in finite deformation problems. Int. J. Solids Struct. 20, 725–737.

Khan, A.S., Huang, S.J., 1995. Continuum Theory of Plasticity. Wiley, New York.

Kuroda, M., 1997. Interpretation of the behavior of metals under large plastic shear deformations: a macroscopic approach. Int. J. Plasticity 13, 359–383.

Kuroda, M., 1999. Interpretation of the behavior of metals under large plastic shear deformations: comparison of macroscopic predictions to physically based predictions. Int. J. Plasticity 15, 1217–1236.

Kuroda, M., Tvergaard, V., 2000. Forming limit diagrams for anisotropic metal sheets with different yield criteria. Int. J. Solids Struct. 37, 5037–5059.

Lee, E.H., Mallett, R.L., Wertheimer, T.B., 1983. Stress analysis for anisotropic hardening in finite deformation plasticity. J. Appl. Mech. 50, 554–560.

Lehmann, Th., 1972a. Anisotrope plastische Formänderungen. Romanian J. Tech. Sci. Appl. Mech. 17, 1077–1086.

Lehmann, Th., 1972b. Einige Bemerkungen zu einer allgemeinen Klasse von Stoffgesetzen für große elastoplastische Formänderungen. Ing.-Arch. 41, 297–310.

Loret, B., 1983. On the effect of plastic rotation in the finite deformation of anisotropic elastoplastic materials. Mech. Mater. 2, 287–304.

Lubarda, V.A., 1988. Simple shear of a strain-hardening hollow circular cylinder. Int. J. Plasticity 4, 61–73.

Majors, P., Krempl, E., 1994. Comments on induced anisotropy, the Swift effect, and finite deformation inelasticity. Mech. Res. Commun. 21, 465–472.

Metzger, D.R., Dubey, R.N., 1987. Corotational rates in constitutive modelling of elastic–plastic deformation. Int. J. Plasticity 4, 341–368.

Montheillet, F., Cohen, M., Jonas, J.J., 1984. Axial stress and texture development during the torsion testing of Al, Cu and α-Fe. Acta Metall. 32, 2077–2089.

Moss, C., 1984. On instabilities in large deformation simple shear loading. Comp. Mech. Appl. Mech. Engng. 46, 329–338.

Nagtegaal, J.C., de Jong, J.E., 1982. Some aspects of non-isotropic work-hardening in finite strain plasticity. In: Lee, E.H., Mallett, R.L. (Eds.), Plasticity of Metals at Finite Strain: Theory, Experiment and Computation, Stanford University, USA, pp. 65–102.

Nayfeh, A., 1973. Perturbation Methods. Wiley, New York.

Neale, K.W., 1981. Phenomenological constitutive laws in finite plasticity. SM Archives 6 (1), 79–128.

Nemat-Nasser, S., 1983. On finite plastic flow of crystalline solids and geomaterials. J. Appl. Mech. 50, 1114–1126.

Nemat-Nasser, S., 1992. Phenomenological theories of elasto-plasticity and strain localization at high strain rates. Appl. Mech. Rev. 45, S19–S45.

Ning, J., Aifantis, E.C., 1994a. On anisotropic finite deformation plasticity. Part I. Acta Mechanica 106, 55–72.

Ning, J., Aifantis, E.C., 1994b. On anisotropic finite deformation plasticity. Part II. Acta Mechanica 106, 73–85.

Paulun, J.E., Pecherski, R.B., 1985. Study of corotational rates for kinematic hardening in finite deformation plasticity. Arch. Mech. 37, 661–678.

Reed, K.W., Atluri, S.N., 1985. Constitutive modelling and computational implementation for finite strain plasticity. Int. J. Plasticity 1, 63–87.

Simo, J.C., Pister, K.S., 1984. Remarks on rate constitutive equations for finite deformation problem: computational implications. Compt. Meth. Appl. Mech. Engng. 46, 201–215.

Szabó, L., Balla, M., 1989. Comparison of stress rates. Int. J. Solids Struct. 25, 279–297.

Tsakmakis, Ch., Haupt, P., 1989. On the hypoelastic-idealplastic constitutive model. Acta Mechanica 80, 273–285.

Xia, Z., Ellyin, F., 1993. A stress rate measure for finite elastic plastic deformation. Acta Mechanica 98, 1–14.

Xiao, H., Bruhns, O.T., Meyers, A., 1997a. Logarithmic strain, logarithmic spin and logarithmic rate. Acta Mechanica 124, 89–105.

Xiao, H., Bruhns, O.T., Meyers, A., 1997b. Hypo-elasticity model based upon the logarithmic stress rate. J. Elasticity 47, 51–68.

Xiao, H., Bruhns, O.T., Meyers, A., 1998a. On objective corotational rates and their defining spin tensors. Int. J. Solids Struct. 35, 4001–4014.

Xiao, H., Bruhns, O.T., Meyers, A., 1998b. Strain rates and material spins. J. Elasticity 52, 1–42.

Xiao, H., Bruhns, O.T., Meyers, A., 1999. On the existence and uniqueness of the integrable-exactly hypoelastic equation $\mathring{\boldsymbol{\tau}}^{*} = \lambda(\mathrm{tr}\mathbf{D})\mathbf{I} + 2\mu\mathbf{D}$ of grade zero and its significance to finite inelasticity. Acta Mechanica 138, 31–50.

Yang, W., Cheng, L., Hwang, K.C., 1992. Objective corotational rates and shear oscillation. Int. J. Plasticity 8, 643–656.

Zbib, H.M., Aifantis, E.C., 1988a. On the concept of relative and plastic spins and its implications to large deformation theories. Part I. Acta Mechanica 75, 15–33.

Zbib, H.M., Aifantis, E.C., 1988b. On the concept of relative and plastic spins and its implications to large deformation theories. Part II. Acta Mechanica 75, 35–56.